EFDA–JET–PR(11)42

O.J. Kwon, I.T. Chapman, P. Buratti, H. Han
and JET EFDA contributors

Stability Analysis of High Beta Plasmas in JET

Stability Analysis of High Beta Plasmas in JET

O.J. Kwon[1], I.T. Chapman[2], P. Buratti[3], H. Han[4]
and JET EFDA contributors*

JET-EFDA, Culham Science Centre, OX14 3DB, Abingdon, UK

[1]Department of Physics, Daegu University, Gyeongbuk 712-714 Korea
[2]EURATOM-CCFE Fusion Association, Culham Science Centre, OX14 3DB, Abingdon, OXON, UK
[3]Associazione EURATOM-ENEA sulla Fusione, C.R. Frascati, Roma, Italy
[4]National Fusion Research Institute, Daejeon 305-806 Korea
** See annex of F. Romanelli et al, "Overview of JET Results",*
(23rd IAEA Fusion Energy Conference, Daejon, Republic of Korea (2010)).

Preprint of Paper to be submitted for publication in
Plasma Physics and Controlled Fusion

ABSTRACT

The linear stability of ideal instabilities with low toroidal mode numbers has been assessed for various high beta plasmas in JET with the minimum in safety factor near 1, 3/2 and 2. In all cases, the plasmas are found to become unstable to global ideal kink-ballooning modes as the minimum safety factor approaches rational values. The plasmas are found to exhibit continuous modes experimentally which degrade performance, with the mode onset being extremely well correlated to the crossing of the numerically-predicted stability boundaries. The most favourable profiles for global stability have also been assessed.

1. INTRODUCTION

In order to achieve steady-state burning plasmas it is necessary to maximise the triple product $nT\tau_E = \beta \tau_E B^2$ where β is the ratio of plasma energy to magnetic field energy $\beta = 2\mu 0 <p> / B_0^2$ and <…> represents an averaging over a flux surface, n,T,p are the plasma density, temperature and pressure respectively, τ_E is the energy confinement time and B is the toroidal magnetic field. Simultaneously, it is necessary to minimize the amount of power required to supply the current non-inductively. `Steady state scenarios' [1-5] aim to maximise the self-generated non-inductively driven bootstrap current [6] by operating at high plasma pressures and low plasma current. However, the energy confinement degrades with plasma current, and consequently an optimization must be reached. Further, high plasma pressures and low currents can lead to MagnetoHydroDynamic (MHD) instabilities which would not be unstable with conventional H-mode profiles [7]. Consequently, it is of great importance to understand the limits of operation set by MHD instabilities in order to tailor plasma profiles accordingly.

The two main candidate scenarios for continuous tokamak operation are the Advanced Tokamak (AT) steady-state scenario [5], which has reversed magnetic shear in the core, low internal inductance and typically β above the no wall limit ; and the `hybrid' stationary scenario [8,9], which has a broad low magnetic shear region with the safety factor, q, above unity, a moderate internal inductance, operating near to the no-wall limit, where the magnetic shear is $s = r/q\ dq/dr$. The reversed shear or broad low shear in the case of the hybrid scenario is a consequence of the optimised non-inductively driven currents, both from auxilliary current drive actuators and from the bootstrap current which is naturally driven off-axis in regions of strong pressure gradients. Combining such broad current profiles with the peaked pressure profiles required for enhanced plasma performance, can result in increased susceptibility to ideal n=1 kink-ballooning modes, or `infernal modes' [7,10]. Whilst these instabilities can be avoided by specific tailoring of the plasma profiles and careful navigation of trajectories in operational space, it is important to understand the domains of operation where such MHD instability will occur.

High beta conditions have been widely explored on JET using both AT and hybrid safety factor profiles. A range of MHD instabilities are encountered, including fast-particle driven chirping modes, tearing modes, and ideal saturated kink modes. It is the latter which is considered here.

Slowly growing (typically 0.2s from birth to saturation) internal modes have recently been found to limit performance in a range of high-beta discharges in JET [11,12], in a similar way to long-living saturated internal instabilities in MAST [13,14] and NSTX [15]. In section 2 we discuss how the JET equilibria are reconstructed, before showing stability analysis of these high beta JET plasmas in section 3 and discussing the implications in section 4.

2. EQUILIBRIUM RECONSTRUCTION

A range of high beta plasmas have been developed in JET, including the steady-state reversed shear scenario [16] and the low-shear hybrid scenario [17]. Furthermore, the beta limit has been approached for a range of q-profiles and minimum safety factors [18]. During the JET high beta experiments, various MHD modes including chirping, kink and tearing modes have observed [11]. Here, our study is mainly focused on shots limited by $n = 1$ MHD instabilities.

The plasma equilibria have been reconstructed at many timeslices for a number of discharges by constraining the EFIT equilibrium reconstruction [19] with MSE field line pitch angle measurements and the magnetic probe measurements. The current profile and plasma shape (with the final closed flux surface taken at $\Psi_N = 0.99$) are then supplied to the HELENA equilibrium code [20] together with the pressure profile shape derived from the high resolution Thomson scattering measurements of the electron temperature and density. The linear stability of these equilibria is then tested using the MISHKA-1 linear stability code [21].

The purpose of this paper is to investigate the evolution of the $n = 1$ ideal MHD stability boundary to determine the stability of experimental equilibrium during the high beta discharge. The effect of the plasma boundary shape, the pressure and current profiles on the stability boundary for different shots and at different time slices for the same shot is also studied.

3. STABILITY CALCULATION

3.1 $q_{min} \approx 3/2$

For JET Pulse No: 77877, the weak chirping mode appears at 5.8sec and the continuous (long-lived) $n = 1$ kink mode starts at 6.2sec. Both β_N and β_p increase until the continuous mode appears and peaks at 2.6 and 1.4, respectively, at the time of the appearance of the mode as shown in Fig.1. They then decrease as the existence of the continuous mode seriously degrades the energy confinement. The central q generally decreases with time and $q_{min} \approx 1.7$ at 6.2sec.

The growth rate contour plot for the Pulse No: 77877 at 6.2 for the $n = 1$ no wall mode is shown in Fig.2. This plot is constructed by performing hundreds of stability analyses with variations in q_{min} and β_p. During the stability scan, the normalized pressure and current profiles are kept constant while β_p and q_0 are independently varied. The minimum safety factor is varied by scaling the toroidal field whilst keeping the pressure constant, whilst β_p is varied by scaling the pressure on-axis for the same pressure profile and toroidal field. Of course this means that there are variations in the resultant consistent equilibria, and so only the reconstructions near the experimental conditions are

really representative of JET plasmas. However, we retain the wide variation in pressure and safety factor to help to explicate how one may attempt to traverse operating parameter space and avoid saturated core instabilities of the type shown in figure 1.

The experimental equilibrium point is shown here as red square and it lies in the unstable region. Note that the continuous mode is experimentally first observed at this time. Higher β_p can be achieved without destabilizing the n = 1 instability when q_0 is raised. However, when the contour plot is plotted as a function of β_N instead of β_p, there is not much improvement of stability when q_0 is increased and the mode is even destabilized at slightly lower β_N at higher q_0. This can be seen in figure 3 where the same stability boundary as for figure 2 is now plotted in respect of β_N. The eigenfunction plot of the experimental equilibrium of the shot 77877 at 6.2sec, shown in Fig. 4, has dominant internal m = 2, 3, and 4 components as well as considerable contribution from higher m external kink components. The equilibrium is reconstructed at 6.2s as the experimental time when the pressure is maximized, though the eigenfunction does not change significantly during other times of instability.

One can see that a structure appears in the stability boundary of Fig.2. This is due to the passing of the integer value of edge q as q_0 is raised for a fixed β_p as shown in Fig.5. When q_a is just above the integer value ($q_a = 5$ in this case for $\beta_p = 1.25$) γ decreases rapidly. Then, γ reaches its local maximum when $q_a \approx 5.5$, before it decreases again. This is due to peeling mode instabilities which are the most unstable mode found by linear eigenvalue analysis when the global n = 1 continuous mode approaches marginal stability, and as such this structure in the stability boundary, whilst interesting, is not of concern.

We can determine the stability boundary at each time slice we have chosen and its change in time is shown in Fig.6. A trajectory of experimental equilibrium is also shown in this Figure. The reconstructed equilibrium stays in the stable region before 5.5sec. It enters the unstable region from the stable region between 5.5sec and 5.9sec. During this time, the stability boundary changes considerably such that the unstable region widens. At the same time, the global equilibrium quantities, especially β_p, also change. It enters the unstable region just before the continuous n = 1 MHD mode is experimentally observed at 6.2sec. This behavior is observed in many other shots. It stays in the unstable region and then makes transition back to the stable region between 6.2sec and 6.6sec when MHD activity is continuously observed experimentally. At this later stage, it has entered the nonlinear phase and cannot be interpreted with linear ideal stability calculations. Nonlinear calculation is beyond the scope of this study. It is remarkable that ideal MHD stability analysis can reproduce this temporal crossing of the stability boundary to be well correlated to the empirical observation of the continuous mode in a number of similar JET plasmas.

To determine what affects the stability boundary, we have compared two equilibia, one at 6.2sec and the other at 6.6sec. The results are shown in Fig.7. Note that the stability boundary of 6.6sec has a wider stable region and the reconstructed equilibrium is in the stable region. When two shapes of the chosen last closed flux surface have been interchanged, i.e, when the plasma boundary of 6.6sec

is used for that of 6.2sec with other quantities or profiles fixed and vice versa, the effect is found to be negligible as seen in Fig.6. When only pressure profile of 6.6sec is replaced by that of 6.2sec, the stability deteriorates from the blue line to the green line in Fig.7. Considering that the pressure profile of 6.6sec (shown in blue in Fig.7(a)) is slightly more peaked than that of 6.2sec, the general understanding that the broader pressure profile is more stable does not apply here. However, the difference in broadness is negligible. The stability also deteriorates when the only current profile of 6.2sec, therefore q and the magnetic shear profiles, replaces that of 6.6sec, as shown in Fig.7. The shear of 6.6sec (shown in blue in Fig.8(b)) is similar to that of 6.2sec for $\sqrt{\Psi_N} < 0.95$, but is larger outside. This helps stabilizing external high m harmonics. Therefore, the stabilizing effects of pressure and current profiles of 6.6sec are combined to have broader stable region at this time compared that of 6.2sec.

We have applied the same method to investigate the transition from stable 5.5sec equilibrium to unstable 5.9sec equilibrium. We have found the same result that both the pressure profile and the current profile act to deteriorate the stability boundary while the plasma boundary shape has little effect during the transition. Whilst one may naively consider the shear in the edge q-profile as an indicator of global stability, the finding that the more unstable 5.9sec equilibrium has larger edge shear than the more stable case of 5.5sec, indicates that the stability boundary can only really be found by reconstructing the plasma with shape and all profiles in greatest fidelity to the experiment.

The conducting wall stabilization has a strong effect when the eigenfunction has considerable external components, for example as in Fig.4. We have shown the effect of a conformal ideally conducting wall for an unstable equilibrium of the Pulse No: 77877 at 6.2sec in Fig.9. It suggests that the wall stabilizes the $n = 1$ mode when $q_{min} > 1.1$ for $r_w = 1.3a$ and when $q_{min} > 1.0$ for $r_w = 1.1a$. The mode is found to be unstable at extremely large q_{min} in figure 9 seen when the conducting wall is far from the plasma though its character is changed to become far more edge localized. This behaviour is not thought to be of concern in real JET plasmas in the presence of a close fitting wall. The JET wall has been shown to have an approximately equivalent effect to assuming a wall at $r_w = 1.3a$ [23], meaning that the minimum safety factor required to avoid such internal modes is $q_{min} > 1.1$ at the relatively high β_N achieved in these JET discharges.

3.2 $q_{min} \approx 2$

For the Pulse No: 72546, the continuous $n = 1$ kink mode starts at 3.5sec without the appearance of the chirping mode, and disappears at 4.2sec. The maximum $\beta_p \approx 2.3$ is achieved at 3.3sec at relatively high $q_0 \approx 2.1$. A trajectory of experimental equilibrium and calculated ideal MHD stability boundaries are shown in Fig. 10. During the transition from the stable equilibrium of 2.9sec to the unstable equilibrium of 3.8sec, the equilibrium quantities generally moves to less favorable region, such that β_p increases and q_0 decreases. The ideal MHD stability boundary improves during this period, on the contrary to that of the Pulse No: 77877. However, the improvement is not enough and the equilibrium of 3.8sec becomes marginally unstable.

A structure in the stability boundaries is more apparent for this shot, because it has more contribution from large m edge components. For $\beta_p = 1.1$, the equilibrium is locally most unstable when q_a is half integer (3.5, 4.5, 5.5) and is locally least unstable for integer values of q_a (4 and 5) as seen in Fig.11. The effect of the ideal wall is also more pronounced for the more external higher m harmonics of the eigenfunction.

3.3 $q_{min} \approx 1$

The stability boundaries of Pulse No: 73751, which has $q_{min} \approx 1$, are quite different from those of Pulse No's: 77877 and 72546. Rigid low q_0 limits exist as shown in Fig.12. Experimentally, the continuous n = 1 MHD activity starts with higher frequency of 13kHz from 5.0sec and later with lower frequency of 5kHz and decreasing frequency from 7.7sec. The continuous mode does not appear until relatively high $\beta_N \approx 3.1$ and relatively low $q_0 \approx 1.2$ is achieved. From Fig.12, one can see that the reconstructed experimental equilibrium is marginally stable at 5.0sec and marginally unstable for 6.0sec. The mode structure of the unstable 7.0sec shows a large internal m = 1 component and relatively insignificant contribution from higher m components, as illustrated in figure 13. Therefore, the conducting wall stabilization is less effective in this case.

Equilibrium conditions are compared to investigate the difference in the stability boundary between shots. In Fig.14, the Pulse No: 73751 at 6sec and the Pulse No's: 77877 at 6.2sec are chosen for comparison. The stability boundary of the latter is generally more unstable. When the plasma boundary of the former is used for the equilibrium reconstruction of the latter with p' and j profiles unchanged, the stability boundary even worsens from the red line to the purple line in Fig.14.

The plasma boundary of the Pulse No: 73751 is less elongated and less shaped than that of Pulse No: 77877 as shown in Fig.15. Therefore, more shaped plasma acts to stabilize the mode as expected. However, effect of p' and j profiles of the Pulse No: 73751 is stabilizing enough to overcome the destabilizing effect of the plasma boundary shape. When only p' of the Pulse No: 77877 is replaced by that of the Pulse No: 73751, the n=1 stability boundary improves considerably from the red curve to the green curve in Fig.14, almost similar to the stability boundary of more stable Pulse No: 73751. This also applies when only j profile of Pulse No: 77877 is replaced by that of Pulse No: 73751. Therefore, the favorable effect of broad pressure profile and peaked current profile of the Pulse No: 73751, as seen in Fig.16 combine to produce widened stable region. The internal inductance for the Pulse No's: 73751 and 77877 are 0.88 and 0.67, respectively. It is however worth reiterating that true stability limits cannot be inferred from considering only global parameters like the 3.4li limit assumed in figure 1 to guide the reader.

CONCLUSION AND DISCUSSION

We have analyzed the n = 1 ideal MHD stability properties of recent JET high-beta shots which exhibit global MHD instabilities experimentally, using the MISHKA code. Among a subset of a large number of high-beta pulses in steady-state and hybrid advanced scenarios that we have analyzed,

here we have presented results of 3 cases which have q_0 at the mode onset of 1.0 (Pulse No: 73751), 1.5 (Pulse No: 77877), and 2.0 (Pulse No: 72546), respectively.

The n = 1 ideal MHD stability boundary has been calculated by changing β_p and q_0 with fixed p' and j profiles at some time slices of each shot. This involves reconstructing equilibria and performing stability analyses for hundreds of different equilibria in order to entirely describe the β_p-q_0 space around the experimental point. This allows us to use linear stability analysis to examine the temporal trajectory of the plasma through operating space. The stability boundary is found to change considerably in time. The trajectory of the no-wall stability boundary compared to the operating conditions of different reconstructed equilibria shows that the plasma enters the unstable region just before the onset of the continuous n = 1 MHD mode activity in many cases. This demonstrates that ideal MHD represents a valid description of the plasma for predicting the onset of global long-lived instabilities in plasmas with broad low-shear q-profiles, as seen also in MAST [14].

We have also examined the effect of the plasma shape, p' and j profiles on the stability between different time slices of the same pulse and between different pulses. In general, broader pressure profile, peaked current profile, and more shaped plasma are favorable for the stability but not always. More detailed nuances of the profiles can also be important in determining stability boundaries. Typically the stability boundary contour plots show that as the current diffuses and the safety factor drops, the β_p stability limit also drops, indicating that in principle higher safety factor should be optimal for stable operation to such long-living internal instabilities. However, the highest performance operating scenario was actually attained with minimum safety factor slightly above unity. This is explained by figure 14 which shows a relative invariance of the β_p limit provided q_{min} is above a critical value just above one. In this case, the broader pressure and peaked current density profiles are the key to improved stability. This suggests that optimal performance with elevated safety factor may also be attained by tailoring the pressure and current profiles in such a fashion to be similar to this hybrid plasma.

Finally, the phase and displacement profiles from the MISHKA results and ECE measurement have also been compared in order to test whether the reconstructed equilibria are representative of the experimental plasmas. The result shows very good agreement in the core region of plasma. Details of this comparison can be found elsewhere [11].

ACKNOWLEDGEMENT

Authors, O. Kwon and H. Han, would like to thank the support by National R&D Program through the National Research Foundation of Korea (NRF) funded by the Ministry of Education, Science and Technology(2011-0018732). This work, supported by the European Communities under the contract of Association between EURATOM and CCFE, was carried out within the framework of the European Fusion Development Agreement. The views and opinions expressed herein do not necessarily reflect those of the European Commission. This work was also part-funded by the RCUK Energy Programme under grant EP/I501045.

REFERENCES

[1]. Becoulet A. and Hoang G.T, 2008 *Plasma Physics and Controlled Fusion* **50** 124055

[2]. Litaudon X et al, 2007 *Plasma Physics and Controlled Fusion* **49** B529

[3]. Joffrin E, 2007 *Plasma Physics and Controlled Fusion* **49** B629

[4]. Doyle E.J. et al, 2006 *Plasma Physics and Controlled Fusion* **48** B39

[5]. Taylor T.S 1997 *Plasma Physics and Controlled Fusion* **39** B47

[6]. Bickerton R.J. et al, 1971 *Nature Physics Science* **229** 110

[7]. Manickam J. et al, 1994 *Physics of Plasmas* **1** 1601

[8]. Sips A.C.C. et al, 2005 *Plasma Physics and Controlled Fusion* **47** A19

[9]. Joffrin E, 2005 *Nuclear Fusion* **45** 626

[10]. Manickam J et al, 1987 *Nuclear Fusion* **27** 1461

[11]. Buratti P et al, 2011 *sub Nuclear Fusion*

[12]. Buratti P et al, 2009 36th EPS Conference on Plasma Physics, Sofia O2.007 ``MHD stability limit analysis in JET high beta advanced scenarios'' and http://epsppd.epfl.ch/Sofia/start.htm

[13]. Chapman I.T et al 2010 *Nuclear Fusion* **50** 045007

[14]. Chapman I.T et al, 2011 *Nuclear Fusion* **51** 073040

[15]. Menard J.E et al, 2006 *Physics Review Letters* **97** 095002

[16]. Mailloux J et al, 2010 Proc 23rd Fusion Energy Conference, Daejon, Korea, EXC/1-3

[17]. Hobirk J et al, 2009, 36th EPS Conference on Plasma Physics, Sofia, Bulgaria, O5.057

[18]. Challis C et al 2009 36th EPS Conference on Plasma Physics P5.172 "Stability and confinement optimisation in the range q_0=1-3 at JET'' and http://epsppd.epfl.ch/Sofia/start.htm

[19]. Lao L et al, 1990 *Nuclear Fusion* **30** 1035

[20]. Huysmans G, Goedbloed J. and Kerner W. 1991 Proceedings of the CP90 Conference on Computer Physics, (World Scientific, Singapore), p. 371

[21]. Mikhailovskii A.B, Huysmans G.T.A, Sharapov S.E. and Kerner W.O. 1997 *Plasma Physics Report* **23** 844

[22]. Gryaznevich M.P et al 2008 *Plasma Physics and Controlled Fusion* **50** 124030

[23]. Chapman I.T et al, 2009 *Plasma Physics and Controlled Fusion*, **51**, 055015

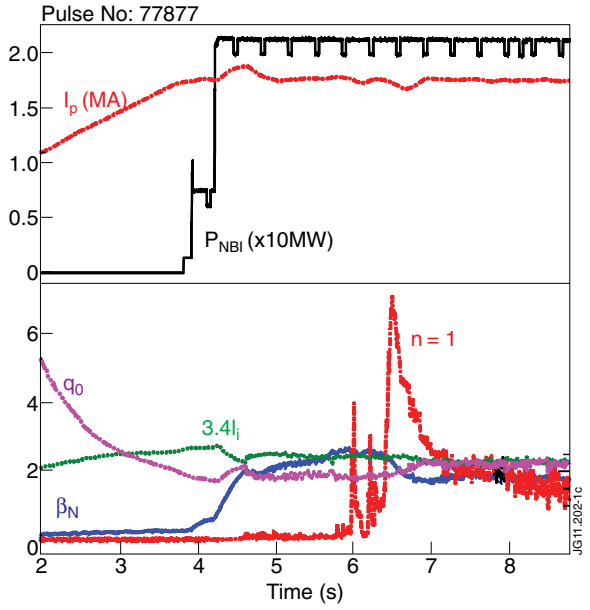

Figure 1: The timetraces for JET Pulse No: 77877 showing typical continuous mode onset. (Top) The plasma current and injected beam power are ramped up and held constant (Bottom) The normalized beta rises through the shot above the 3.4li level previously assumed to be a good estimate of the no-wall limit in JET [22]. After some n = 1 fast ion driven chirping behaviour the continuous mode onset occurs at 6.2s when the safety factor reaches its minimum value and the β_N collapses.

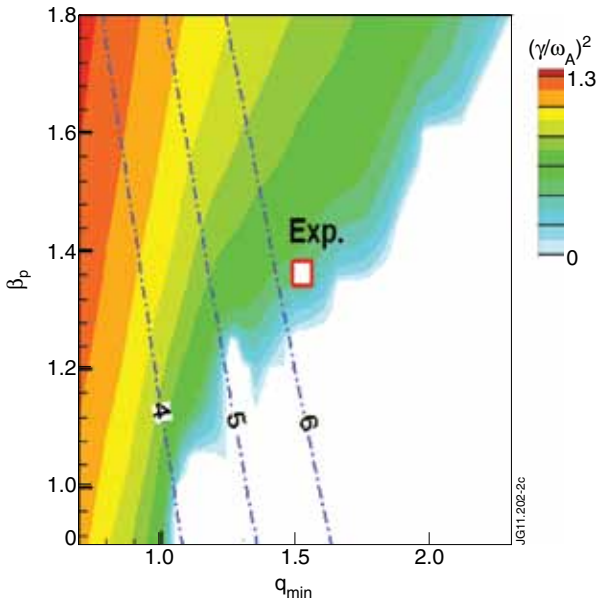

Figure 2: Growth rate contour plot of Pulse No: 77877 at 6.2sec. The dashed lines show stability boundaries set by rational safety factor surfaces at the plasma edge.

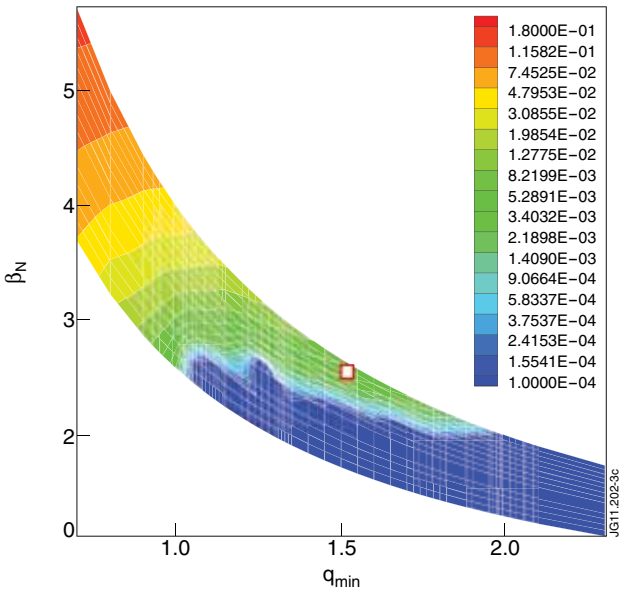

Figure 3: Growth rate contour plot of Pulse No: 77877 at 6.2s, as in figure 2, but now shown with respect to β_N.

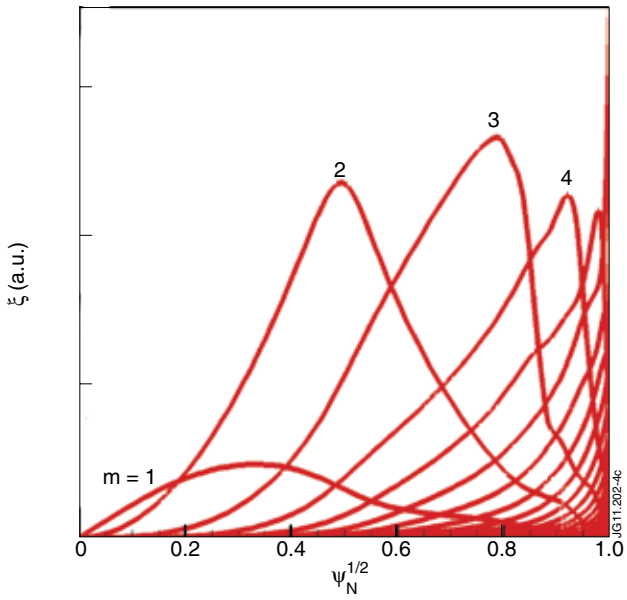

Figure 4: Eigenfunction plot of Pulse No: 77877 at 6.2sec.

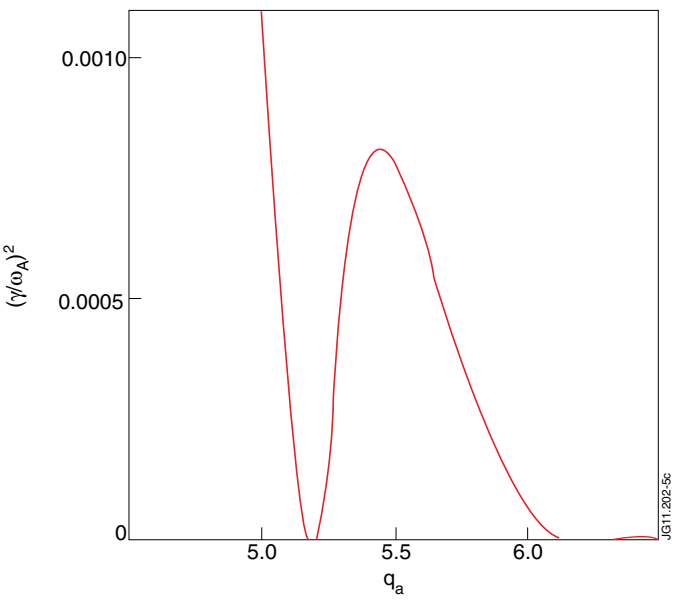

Figure 5: Eigenvalue as a function of qa for β_p = 1.25 based on equilibrium of Pulse No: 77877 at 6.2sec. Here, local maximum appears at $q_a \approx 5.5$.

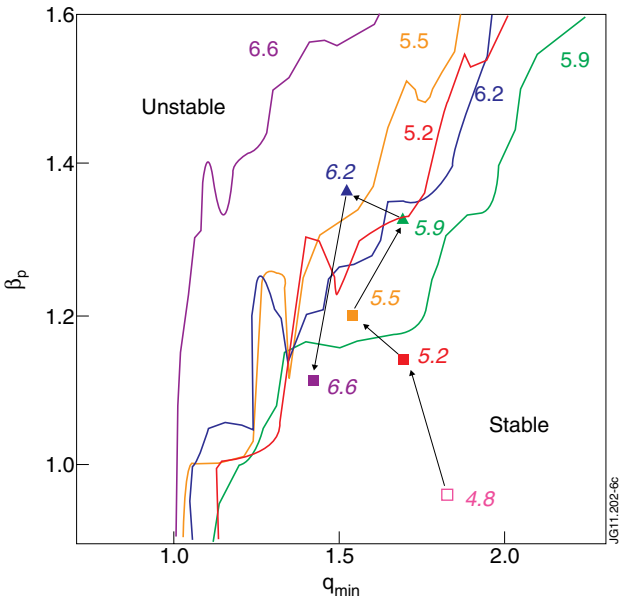

Figure 6: MHD stability boundaries and a trajectory of experimental equilibrium in $\beta_p - q^{min}$ space for Pulse No: 77877. Numbers correspond to different time slice.

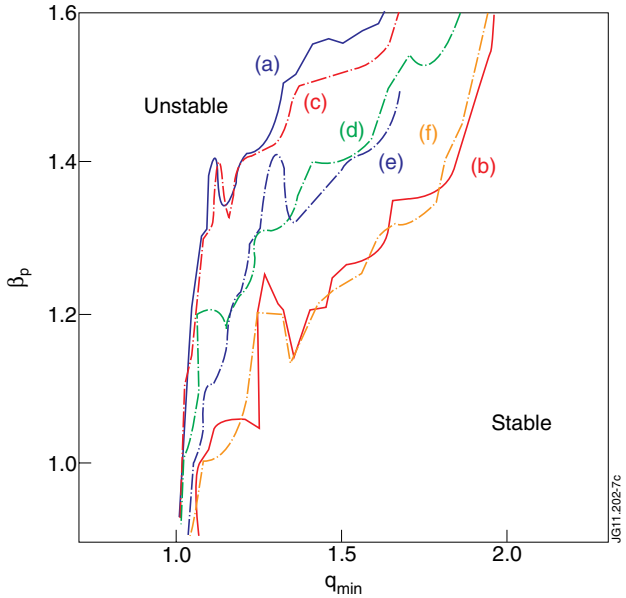

Figure 7: Effect of p' and J profiles of Pulse No: 77877 at 6.2sec and at 6.6sec on stability boundaries. (a) The blue and (b) red curves show the stability boundary at 6.2s and 6.6s respectively, whilst dashed curves show the boundaries when the equilibrium from 6.6s is reformulated with either (c) the boundary, (d) pressure profile or (e) current profile from 6.2s in order to assess the driving feature in determining instability. The dashed curve (f) is when the equilibrium of 6.2s is reformulated with the boundary of 6.6s.

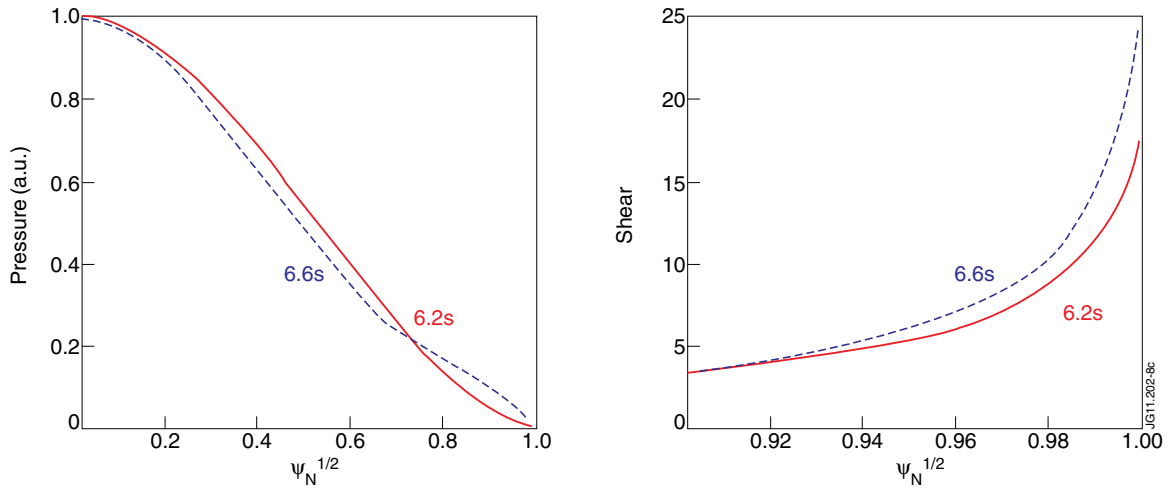

Figure 8: (a) pressure and (b) shear of Pulse No: 77877 at unstable 6.2sec in red and stable 6.6sec in blue for $\beta_p = 1.25$.

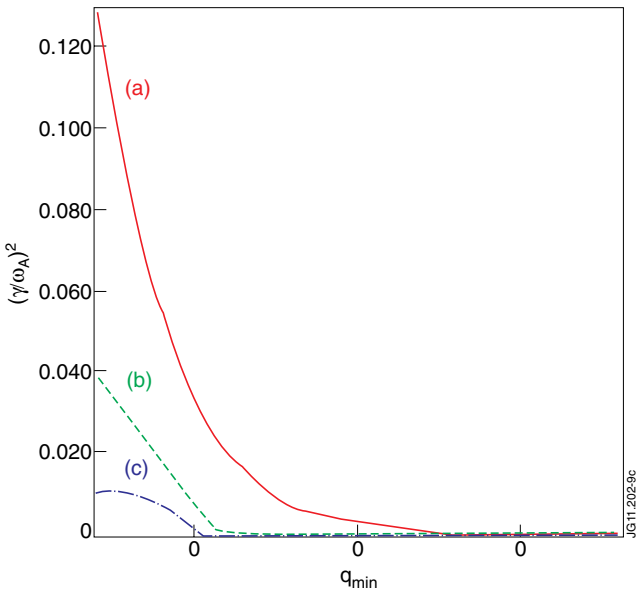

Figure 9: Effect of the conformal conducting wall for Pulse No: 77877 at 6.2sec with the relative wall radius of (a) 10.0a (b) 1.3a and (c) 1.1a. The real JET wall has approximately equivalent effect to a conformal wall at 1.3a.

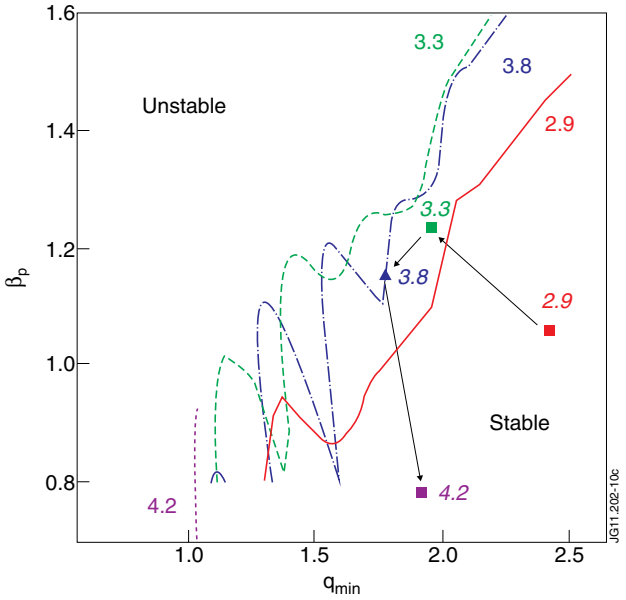

Figure 10: MHD stability boundaries and a trajectory of experimental equilibrium in $\beta_p - q_{min}$ space for the Pulse No: 72546. Numbers correspond to different time slice.

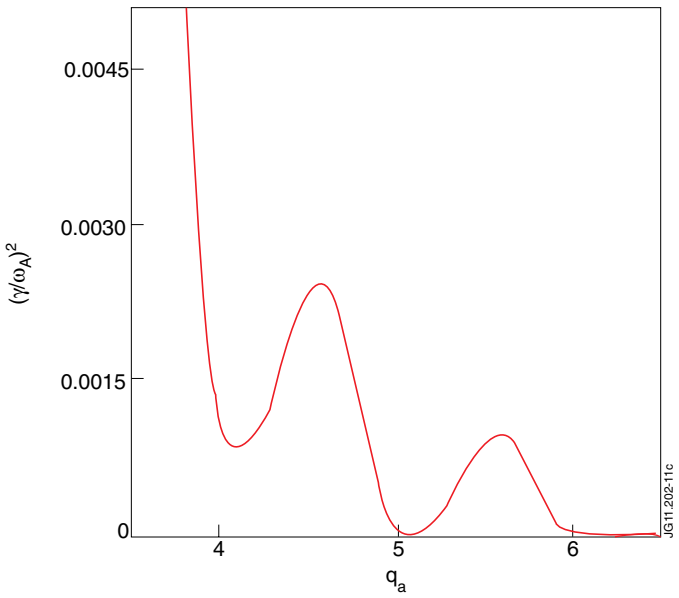

Figure 11: Eigenvalue as a function of qa for $\beta_p = 1.1$ based on equilibrium of Pulse No: 72546 at 3.8sec.

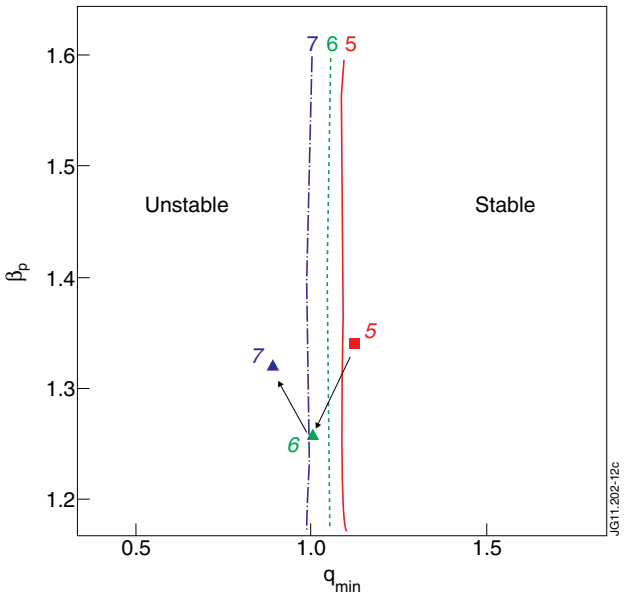

Figure 12: MHD stability boundaries and a trajectory of experimental equilibrium in $\beta_p - q_{min}$ space for the Pulse No:73751. Numbers correspond to different time slice.

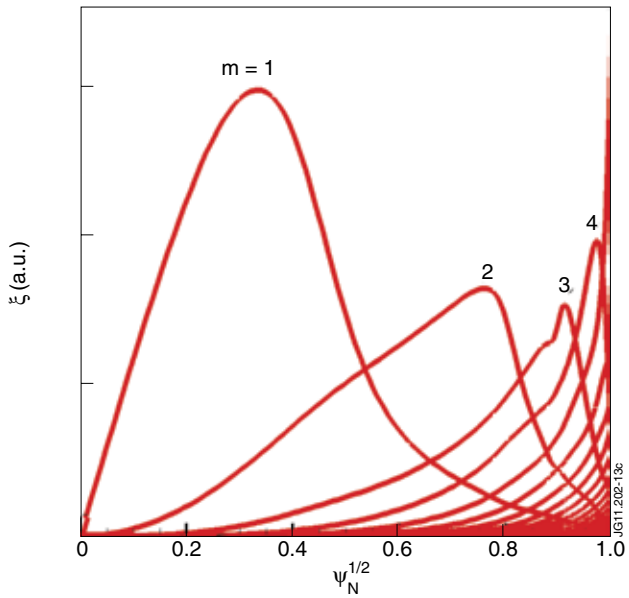

Figure 13: Eigenfunction plot of Pulse No: 73751 at 7sec.

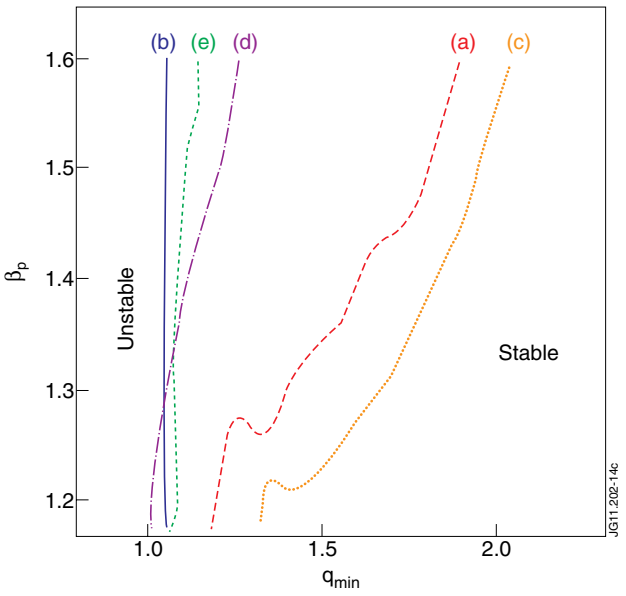

Figure 14: Effect of p' and J profiles of Pulse No: 77877 at 6.2sec and Pulse No: 73751 at 6.0sec on stability boundaries. (a) The red and (b) blue curves show the stability boundary of Pulse No's: 77877 and 73751 respectively, whilst dashed curves show the boundaries when the equilibrium from shot 77877 is reformulated with either (c) the boundary, (d) pressure profile or (e) current profile from Pulse No: 73751.

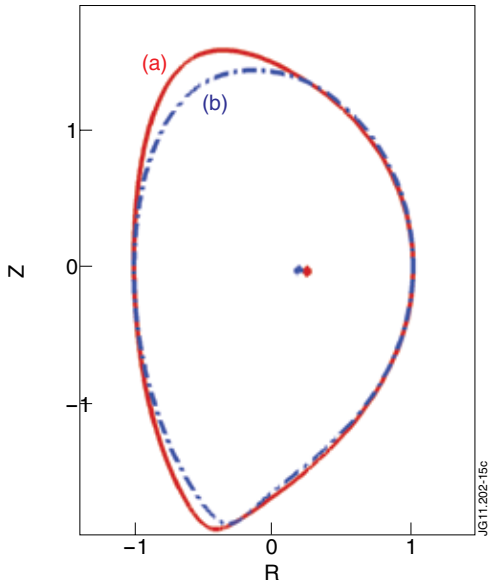

Figure 15: Plasma boundary shapes of Pulse No: 77877at 6.2sec in red and Pulse No: 73751at 6.0sec in blue.

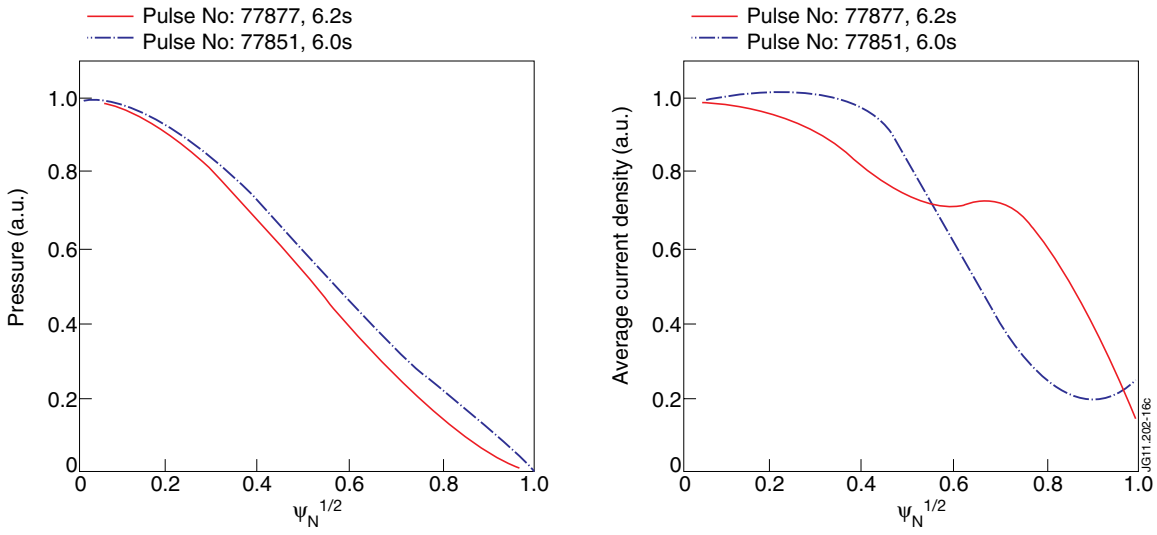

Figure 16: (a) pressure and (b) current profiles of Pulse No: 77877 at 6.2sec in red and Pulse No: 73751at 6.0sec in blue.